

2020-03-17

Responses of Intertidal Bacterial Biofilm Communities to Increasing pCO₂

Kerfahi, D

<http://hdl.handle.net/10026.1/15583>

10.1007/s10126-020-09958-3

Marine Biotechnology

Springer Science and Business Media LLC

All content in PEARL is protected by copyright law. Author manuscripts are made available in accordance with publisher policies. Please cite only the published version using the details provided on the item record or document. In the absence of an open licence (e.g. Creative Commons), permissions for further reuse of content should be sought from the publisher or author.

1
2 This is the author's accepted manuscript. The final published version of this work (the version of record) is published by
3 Springer Nature in *Marine Biotechnology*. The manuscript was made available online on the 17 March 2020 at: [https://](https://doi.org/10.1007/s10126-020-09958-3)
4 doi.org/10.1007/s10126-020-09958-3 This work is made available online in accordance with the publisher's policies. Please
5 refer to any applicable terms of use of the publisher.

6

7 **Responses of intertidal bacterial biofilm communities to increasing $p\text{CO}_2$ in**
8 **a naturally acidified system**

9 Dorsaf Kerfahi¹, Ben Harvey², Sylvain Agostini², Koetsu Kon², Ruiping Huang³, Jonathan M.
10 Adams^{4*}, Jason M. Hall-Spencer^{2,5}

11 ¹School of Applied Biosciences, College of Agriculture and Life Sciences, Kyungpook
12 National University, Daegu, 41566, Republic of Korea.

13 ²Shimoda Marine Research Center, University of Tsukuba, 5-10-1 Shimoda, Shizuoka, Japan.

14 ³State Key Laboratory of Marine Environmental Science, Xiamen University, Xiamen,
15 Fujian, 361100, China.

16 ⁴School of Geographic and Oceanographic Sciences, Nanjing University, Nanjing 210008,
17 China.

18 ⁵School of Biological and Marine Sciences, University of Plymouth, Plymouth, PL4 8AA,
19 United Kingdom.

20

21 ***Corresponding author:** Jonathan M. Adams.

22 School of Geographic and Oceanographic Sciences, Nanjing University, Nanjing 210008,
23 China.

24 E-mail: foundinkualalumpur@yahoo.com

25 **Abstract**

26 The effects of ocean acidification on ecosystems remain poorly understood, because it
27 is difficult to simulate the effects of elevated CO₂ levels on entire marine communities in
28 controlled laboratory conditions. Natural systems such as CO₂ seeps that are enriched in CO₂
29 are being used to help understand the long-term effects of ocean acidification *in situ*. Here,
30 we compared biofilm bacterial community composition on cobbles/boulders and bedrock
31 along a CO₂ gradient in the NW Pacific. Samples sequenced for 16S rRNA showed that
32 different bacterial communities were associated with zones of different seawater *p*CO₂, and
33 were also distinct between the two rocky habitat types. In both habitats, there was increased
34 bacterial diversity in the biofilm communities in acidified conditions. Differences in *p*CO₂
35 were associated with differences in the relative abundance of major bacterial phyla including
36 Cyanobacteria, Bacteroidetes, Proteobacteria, Planctomycetes, and Verrucomicrobia.
37 However, despite the differences in community composition, there is little sign of changes in
38 the bacterial community that would be functionally significant in terms of nutrient cycling
39 and ecosystem structure. As well as direct seawater pH effects, it is possible that increased
40 growth of algae and decreased grazing contributed to the observed shift in bacterial
41 community composition at high CO₂, as documented at several seep systems worldwide.
42 Given the importance of biofilms to coastal ecology, changes in their composition due to
43 globally rising *p*CO₂ levels requires further investigation to assess the implications for marine
44 ecosystem function. However, the apparent lack of functional shifts in the biofilms despite
45 the pH change may be a reassuring indicator of stability in shallow oceanic biofilm
46 communities in the future.

47

48 **Keywords:** Bacteria, biodiversity, ocean acidification, rocky shore ecology.

49 **Introduction**

50 Bacteria dominate the abundance, diversity and metabolic activities of ocean
51 ecosystems (Azam and Malfatti, 2007). On hard substrates they form attached biofilm
52 communities where they interact in a matrix of extracellular polymeric substances (Decho,
53 2000; de Carvalho, 2018), which stick the cells to the substrata and protect them against
54 environmental extremes. Marine biofilms rapidly colonise natural and artificial surfaces, and
55 then facilitate the settlement of macroalgae and invertebrates (Lau et al., 2005; Qian et al.,
56 2007). They cycle nutrients and organic matter, and can be a major source of primary
57 productivity in the photic zone, providing an important food resource for higher trophic
58 levels (Thompson et al., 2004; de Carvalho, 2018). Consequently, any changes in biofilm
59 microbial diversity and abundance could have important implications for marine ecosystem
60 structure and function (Weinbauer et al., 2011).

61 Anthropogenic CO₂ emissions are rapidly changing seawater chemistry, in a process
62 called ocean acidification, and a major research priority is to find out how ecosystems will be
63 affected by these changes (Riebesell and Gattuso, 2015). While marine organisms can
64 tolerate large, rapid changes in carbonate chemistry in coastal regions (Wootton et al., 2008),
65 the long-term effects of decreased mean pH and more frequent episodes of low carbonate
66 saturation and high *p*CO₂ are poorly known. Areas that are naturally exposed to periods of
67 lower pH, lower carbonate saturation and higher *p*CO₂ than those that occurred at pre-
68 industrial levels of atmospheric CO₂ are helping to further our understanding of the
69 ecosystem effects of ocean acidification (Hall-Spencer et al., 2008; Fabricius et al., 2011;
70 Rastrick et al., 2018). This approach has shown that even in coastal ecosystems, where rapid
71 changes in carbonate chemistry are normal, many calcified organisms are adversely affected
72 when the frequency and duration of low carbonate saturation events increase. Concomitant
73 pulses of high levels of dissolved inorganic carbon benefit certain primary producers, causing

74 shifts in their community composition (Porzio et al., 2011; Connell et al., 2013; Cornwall et
75 al., 2017).

76 Ocean acidification may directly impact microbial diversity and composition, and
77 indirectly affect microbes through links within food webs, for example with non-bacterial
78 competitors and with grazers (Krause et al., 2012; Sunday et al., 2017). Despite the
79 importance of microbial biofilms, few studies have investigated how ocean acidification
80 might affect them (Liu et al., 2010; Kerfahi et al., 2014). Hypothetically, major
81 biogeochemical processes driven by microbes may not be fundamentally different under
82 future elevated $p\text{CO}_2$ conditions (Joint et al., 2011) since bacterial communities are able to
83 reorganise themselves in response to environmental perturbations (Tolker-Nielsen and Molin,
84 2000). Aquarium-based experiments have been used to simulate these future conditions, but
85 it is challenging to predict the responses of microbial communities based on these, as they do
86 not incorporate feedbacks and the many indirect effects that might occur as a result of
87 increased $p\text{CO}_2$ in natural systems – for example changes in geochemistry and organism
88 interactions (Das and Mangwani, 2015). For this reason, carbon dioxide seep systems are
89 now being used to investigate the long-term response of microbial communities to ocean
90 acidification (Kerfahi et al., 2014; Morrow et al., 2014; Hassenrück et al., 2015, 2017;
91 O'Brien et al., 2018).

92 Previous work on biofilm communities at carbon dioxide seeps suggests that their
93 primary productivity will be enhanced by ocean acidification in the photic zone, at least
94 where nutrient levels are sufficient (Lidbury et al., 2012; Johnson et al., 2015) and that there
95 will be broad shifts in their community composition and diversity under increased $p\text{CO}_2$
96 (Kerfahi et al., 2014; Taylor et al., 2014). These biofilm community responses have also been
97 shown in mesocosm-based studies using experimentally elevated $p\text{CO}_2$ (Witt et al., 2011)
98 with no evidence of loss of biofilm function due to ocean acidification.

99 Natural biofilm communities on rocky shores are highly variable in terms of
100 community structure and relative abundances, due to abiotic and biotic pressures (Williams et
101 al., 2000), and rocky shore ecology is strongly influenced by shore type e.g. steep cliffs vs
102 boulder fields, or hard vs soft rock substrata (Lewis, 1964). The response of microbial
103 biofilms to the impacts of ocean acidification may differ, depending on habitat type, and may
104 be caused directly by changes in carbonate chemistry, or indirectly due to effects on other
105 organisms (Sunday et al., 2017).

106 In this study, our aim was to test whether the effects on coastal biofilm bacterial
107 communities of increased seawater $p\text{CO}_2$ in the NW Pacific Ocean are similar to those
108 observed in the Mediterranean Sea (Kerfahi et al., 2014). In Japan, Agostini *et al.* (2018)
109 recently showed that in complex habitats, at increased levels of $p\text{CO}_2$ predominately
110 calcareous organisms were replaced by simplified biofilm-dominated and algal turf-
111 dominated habitats. We used the ocean acidification study system established by Agostini *et*
112 *al.* (2018) to investigate the bacterial community structure of these biofilms on two types of
113 low rocky shore habitat; cobble/boulder shores, and steep cliff faces. We examined four
114 $p\text{CO}_2$ conditions, from pre-Industrial through to present day and projected future levels, to
115 assess impacts of changing ocean chemistry on bacterial communities. We expected to find
116 major changes in biofilm community composition, given the known sensitivity of bacterial
117 communities to pH (e.g. Lauber et al., 2008; Tripathi et al., 2012), although this type of study
118 has not previously been carried out in the Pacific Ocean.

119

120 **Materials and methods**

121 **Study site**

122 Sampling took place on the South coast of Shikine Island, East of the Izu peninsula,
123 Japan in the North West Pacific Ocean (34° 32'N, 139° 20'E). The Izu archipelago is a chain

124 of islands approximately 150 km South of Tokyo (Fig. S1) situated at a subtropical-temperate
125 biogeographic boundary due to the influence of the warm North flowing Kuroshio current
126 (Agostini et al., 2018).

127

128 **Sample collection and DNA extraction**

129 Samples were collected from six sites along a pH gradient ranging from 7.2 to 8.3. At
130 each site, six rock chips were randomly collected along a linear 1 m transect immediately
131 above the low tide line. All samples had the same edaphic parameters, being on boulders (in
132 boulder samples) or cliff faces (in cliff face samples) of the same basaltic lava, on flat faces at
133 vertical westerly orientation and smooth texture. Rock chips were collected in June 2016
134 using a chisel and placed in individually labelled bags using clean forceps (Fig. S2) and
135 immediately stored at -20°C. DNA was extracted from each rockchip sample using the Power
136 Soil DNA extraction kit (MO BIO Laboratories, Carlsbad, CA, USA) following the
137 manufacturer's protocol. The DNA samples were then sent to the Dalhousie University,
138 Canada, for sequencing using an Illumina MiSeq platform.

139

140 **Seawater chemistry**

141 Geographical co-ordinates of each sample were taken using a GPS. A multi-sensor
142 (U-5000G, Horiba Ltd, Kyoto Japan) was used to measure seawater pH, temperature, salinity
143 and dissolved oxygen. To measure total alkalinity, 100 ml water samples were collected and
144 then filtered at 0.45 µm with cellulose acetate filters (Dismic 045, Advantec Japan). Total
145 alkalinity was measured via titration with HCl at 0.1 mol l⁻¹ with a Metrohm titrator (785
146 DMP titrino) and total alkalinity was calculated by Gran plot from titration point with a pH
147 between 4.0 and 3.0. Carbonate chemistry parameters: partial CO₂ pressure (*p*CO₂),
148 Aragonite (Ar) and calcite (Ca) saturation state ($\Omega_{\text{aragonite}}$, Ω_{calcite}), and dissolved

149 inorganic carbon (DIC) were calculated using the CO₂SYS software package (Pierrot et al.,
150 2006) using temperature, salinity, pH (NBS scale) and total alkalinity (A_T) with the
151 disassociation constants from Mehrbach et al. (1973), as adjusted by Dickson and Millero
152 (1987), KSO₄ using Dickson (1990), and total borate concentrations from Uppström (1974).
153 The carbonate chemistry for the different sites is presented in Table 1.

154

155 **Sequence analysis**

156 The sequenced data generated from Miseq sequencing was processed using the
157 Mothur platform (Schloss et al., 2009). The sequences were aligned using Mothur (default
158 settings: kmer searching with 8mers and the Needleman–Wunsch pairwise alignment
159 method). Next, they were aligned against the EzTaxon-aligned reference (Chun et al., 2007),
160 and further filtered to remove gaps. Sequences were de-noised using the ‘*pre.cluster*’
161 command in Mothur implemented using a pseudo-single linkage pre-clustering algorithm
162 from Huse *et al.* (2010). Putative chimeric sequences were detected and removed via the
163 Chimera Uchime algorithm contained within Mothur (Edgar et al., 2011) in *de novo* mode,
164 which first splits sequences into groups and then checks each sequence within a group using
165 the more abundant groups as reference. The taxonomic classification was performed using
166 Mothur’s version of the RDP Bayesian classifier, using EzTaxon-e database for each
167 sequence at 80% Naïve Bayesian bootstrap cut-off with 1000 iterations. The sequences used
168 in this study have been deposited in the NCBI Sequence Read Archive under accession
169 number SRP172073.

170

171 **Statistical analysis**

172 All samples were standardised by random subsampling to 13,882 reads per sample
173 using the `sub.sample` command (<http://www.mothur.org/wiki/Sub.sample>) in Mothur.

174 Richness, diversity indices, and rarefaction values were estimated using Mothur. Variation in
175 the relative abundance of the bacterial phyla among the pH zones was tested using two-way
176 ANOVA in R software package 2.14.2, with habitat type and pH level as fixed factors, after
177 testing for normality. We used Tukey's Honest Significant Difference test for pairwise
178 comparisons. We used the same procedure to test whether OTUs richness and diversity
179 indices differed across different pH levels. OTU-based abundance data were first square root
180 transformed to build the Bray-Curtis distance matrix using the `vegdist` function in the `Vegan`
181 package of R (Oksanen et al., 2008). We performed a nonmetric multidimensional scaling
182 (NMDS) plot using the `metaMDS` function in the `vegan` package of R. This used the Bray-
183 Curtis distance matrix to assess patterns in bacterial species composition. A permutational
184 multivariate analysis of variance (PERMANOVA) was performed with 999 permutations
185 using the `Adonis` function in `Vegan` R package to test if bacterial community composition
186 differed significantly by pH levels and habitat type.

187 The rank order nestedness relationship was also calculated on BINMATNEST
188 (Rodríguez-Gironés and Santamaría, 2006) using default input parameters and null models to
189 test whether the community assemblage in each treatment sample was a subset present in
190 another sample. This approach calculates the p-value for rows and column totals and these
191 were reordered following a packed matrix order from high-to-low nestedness as enumerated
192 by (Dong et al., 2016).

193 Bacterial co-occurrence network analysis was conducted following methods given by
194 (Faust and Raes, 2012; Lima-Mendez *et al.*, 2015). For each group, OTUs that appeared in
195 three or less samples were removed. The relative abundance of OTUs was then used to
196 construct networks using Spearman's correlation and Kullback-Leibler dissimilarity methods.
197 Randomization generated permutation and bootstrap distributions, and *p* values were merged
198 by Brown's method and multiple test correlation with Benjamini-Hochberg. Finally, edges

199 with p_{adj} above 0.05 were discarded.

200 The functional composition of the microbial community was analysed using PICRUSt
201 (Langille et al. 2013) on the OTUs generated from the 16S rRNA data. The PICRUSt
202 program requires a biom-formatted OTU table with OTUs assigned to a Greengenes OTU ID.
203 The 16S OTU table was normalized for copies of the 16S rRNA gene and exported as to
204 .biom format for analysis with the software package STAMP (Parks et al 2014). STAMP
205 includes statistical and visualization tools that were used to identify differences in functional
206 potential for the biofilm bacterial communities across different sites along the pH gradient. .
207 Multiple group comparisons of function abundance (KEGG module predictions) were
208 assessed using analysis of variance (ANOVA) followed by *Tukey–Kramer post hoc* tests
209 (confidence interval of 0.95) and reported with corrected P values (Storey’s FDR multiple
210 test correction approach) in STAMP software (Parks et al 2014).

211

212 **Results**

213 We obtained 583,036 good quality sequences from 36 samples after rarefying to
214 13,882 reads per sample, which were classified into 10,296 operational taxonomic units
215 (OTUs) at 97% similarity level. Most samples showed no sign of reaching an asymptote in
216 OTU richness at the total number of reads available in the rarefaction analysis. This means
217 that more sequences would be required to assess the full taxonomic diversity of bacteria
218 within the biofilms (Fig. S3).

219 Alpha diversity of the bacterial community associated with biofilms across different
220 pH levels was calculated using OTU richness and diversity indices. Bacterial OTU richness
221 was significantly different across all intertidal sites at different pH levels, and highest number
222 of OTUs was observed at sites having the lowest pH (Fig. 1). The OTU richness differed
223 significantly by pH level ($F_{2, 30} = 27.05$, $P < 0.001$) and by the interaction between pH and

224 habitat type ($F_{2, 30} = 3.12, P = 0.05$). Similarly, Shannon index differed significantly in
225 relation to pH ($F_{2, 30} = 15.41, P < 0.001$) and the interaction between pH and habitat type ($F_{2,$
226 $30 = 7.01, P = 0.003$), with highest diversity found in sites having the lowest pH (Fig. 1).
227 However, the community diversity did not differ between the boulder and cliff-face habitats
228 (OTU richness: $F_{1, 30} = 0.83, P = 0.36$; and Shannon index: $F_{1, 30} = 0.08, P = 0.77$).

229 The most dominant bacterial sequences recovered in the present study belonged to
230 *Cyanobacteria* and *Bacteroidetes* representing 36% and 34% of total reads, respectively,
231 followed by *Proteobacteria* with 23% of total reads, and less than 3% for each of the
232 following bacterial phyla: *Planctomycetes*, *Verrucomicrobia*, *Chloroflexi*, *Acidobacteria*,
233 *Actinobacteria*, *Gemmatimonadetes* and *Chlorobi*. 3% of sequences remained unclassified.

234 The relative abundances of phyla in the epilithic bacterial community detected along
235 the pH/CO₂ gradient off Shikine Island showed significant variations across different
236 sampling sites except for *Chloroflexi* and *Chlorobi* (Table S1). The strongest shifts were
237 observed in the most abundant bacterial phyla, with a significant decrease in the relative
238 abundance of *Cyanobacteria* at reduced pH sites. The relative abundance of *Bacteroidetes*
239 was decreased at medium and low pH, but then increased at very low pH sites. However,
240 *Proteobacteria* exhibited an increase in relative abundance at low pH then a decrease at
241 extreme low pH sites. The remaining phyla showed either no consistent patterns or no change
242 in abundance across different sites (Fig. 2). The interaction between pH levels and habitat
243 types had a more pronounced effect on bacterial community than only pH level or habitat
244 type. *Cyanobacteria* were influenced by both factors, with lowest abundance was found in
245 boulder zone and sites having lowest pH. *Bacteroidetes* were significantly affected only by
246 pH with their lowest abundance observed at low pH sites for both boulder and cliff-faced
247 sites. However, *Proteobacteria* were significantly affected only by habitat types showing a
248 decrease in relative abundance at boulder sites. The interaction pH levels and habitat types

249 had a significant effect on most of detected phyla including *Verrucomicrobia*, *Acidobacteria*,
250 *Actinobacteria* and *Gemmatimonadetes*. *Planctomycetes* were significantly affected by pH
251 levels, habitat types and the interaction pH levels*habitat types (Fig. 2, Table S1).

252 More than 25 bacterial orders were detected in our sequences (Fig. 3a).
253 *Sphingobacteriales* were the most abundant order, with a relative abundance of 13.8% of
254 total reads but did not differ at both boulder and cliff-face sites along pH gradient. The
255 relative abundance of almost all detected orders significantly differed in relation to at least
256 one of the studied factors (pH level, habitat type, and interaction pH level*habitat type)
257 (Table S2). The orders *Oscillatoriales*, *Cytophagales*, *Alteromonadales*, *Phycisphaerales*,
258 *Kordiimonadales*, *Chromatiales* and *Balneola* were significantly affected by pH level, habitat
259 type and the interaction of pH level and habitat type. However, *Flavobacteriales* (12.5% of
260 total reads) the second common order significantly differed along pH level and the interaction
261 pH level*habitat type and not with habitat type, with highest abundance found at ambient pH
262 for boulder sites and low pH for cliff-face sites. The relative abundance of *Oscillatoriales* and
263 *Vibrionales* was significantly lower at ambient pH for both boulder and cliff sites.
264 Conversely, *Rhodospirillales* and *Sphingomonadales* were significantly greater at low pH for
265 both habitat types. The remaining orders showed no consistent patterns (Fig. 3a).

266 At the family level, the biofilm bacterial communities at both boulder and cliff-face
267 sites along pH gradient were dominated by *Saprospiraceae* (13.1% of total reads),
268 *Flavobacteriaceae* (12% of total reads), *Prochlorotrichaceae* (7.9% of total reads),
269 *Pleurocapsa* family (7.8% of total reads), *Vibrionaceae* (6.1% of total reads), *Rivulariaceae*
270 (3.9% of total reads), etc. and had significant differences across pH level or/and habitat type
271 except for *Saprospiraceae* ($P>0.05$) the most abundant family (Table S3). Most of the
272 detected families showed no consistent pattern in response to pH and/or habitat type (Fig.
273 3b). For example, *Flavobacteriaceae* were higher at ambient pH in boulder sites and at low

274 pH in cliff-face sites. *Prochlorotrichaceae* were lower at ambient pH in both boulder and cliff
275 sites. Only habitat type had a significant effect on *Vibrionaceae* and *Rivulariaceae* where
276 *Vibrionaceae* represented a minor component of boulder sites (0.2% of total reads) and major
277 component of cliff sites (14% of total reads), conversely *Rivulariaceae* were greater in
278 boulder sites (6.5% of total reads) and lower in cliff sites (1.5% of total reads).
279 *Pseudoalteromonadaceae* had also lower relative abundance in boulder sites (<0.01% of total
280 reads) compared with cliff sites (7.5% of total reads). *Pseudoalteromonadaceae* were
281 significantly influenced by pH, habitat type and the interaction pH level*Habitat type, with
282 lower abundance observed at lower pH (Fig. 3b).

283 A non-metric multidimensional scaling (NMDS) using Bray-Curtis distance indicated
284 that both pH levels and habitat type influenced bacterial community composition (Fig. 4). A
285 permutational multivariate analysis of variance (PERMANOVA) results showed that
286 bacterial community composition was not only affected by pH level ($F_{2,29} = 3.54$, $P = 0.001$;
287 Table 2) and habitat type ($F_{1,29} = 8.62$, $P = 0.001$; Table 2), but also by the interaction
288 between pH level and habitat type ($F_{2,29} = 3.65$, $P = 0.001$; Table 2).

289 Nestedness analysis showed that bacterial communities followed a nested structure (p
290 < 0.0001) across different pH levels. We generated a packed matrix order of all samples, in
291 which the nestedness of each sample was categorised from high to low, and the lower ones
292 are nested in the higher ones (Table S4). Samples having the lowest pH in boulder habitat and
293 samples having ambient pH in cliff-face habitat had the lowest rank of nestedness compared
294 to the other sites. Thus, the OTU composition of other sites could be a subset of the bacterial
295 community in the ‘Boulder-very low’ and ‘Cliff-ambient’ sites.

296 Fig. 5 and Fig. 6 illustrated the interactions between taxa across different pH levels.
297 Associations of bacterial taxa at very low pH sites outnumbered low and ambient pH sites, no
298 matter the rock type. Positive edges were higher than negative edges, except for low pH cliff

299 and ambient boulder sites where the number of positive edges was equal with negative edges
300 (Fig. 5). Furthermore, non-random edges distribution with regard to phylum was observed.
301 We found that both intra-phylum and inter-phylum interaction edges of Bacteroidetes were
302 the highest in all samples (Fig. 6).

303 The functional classification based on KEGG module predictions (Fig. S4) revealed
304 that biofilm microbial communities show some a significant shift in most of the functions in
305 Boulder and Cliff sites across different pH levels. Analysis of PICRUSt-predicted functional
306 profiles for methane metabolic pathways suggest a decrease in gene abundance at lower pH
307 for both boulder and cliff sites (Fig. 7a). Sulfur metabolism showed the opposite pattern with
308 greater gene abundance at lower pH (Fig. 7b). The analysis of nitrogen metabolic pathway
309 suggested no significant difference in gene abundance at both habitat types across different
310 pH level (ANOVA, Tukey–Kramer, $P < 0.05$; Fig. 7c). Genes related to energy metabolic
311 pathways increased at lower pH at both boulder and cliff sites (Fig. 7d). Carbon fixation
312 potential in Prokaryotes showed an increase then a decrease in gene abundance related to
313 carbon fixation in Prokaryotes at boulder sites along pH gradient. These genes decreased at
314 medium pH then increased at low pH at cliff sites (Fig. 7e). The opposite pattern was
315 observed for genes related to carbon fixation pathway in photosynthetic organisms (Fig. 7f).

316

317 **Discussion**

318 We found that bacterial community composition in biofilms on two types of rocky
319 shore habitat was affected at CO₂ seeps (Heat map Fig). Pre-industrial, present day and
320 projected future levels of seawater pCO₂ each had their own discrete communities of biofilm
321 bacteria, raising the possibility that the transition from 300-400 ppm CO₂ in ocean seawater
322 over the past 200 years has already affected biofilm communities worldwide. Biofilm
323 growing at even higher than present-day levels of CO₂ increased in bacterial biodiversity.

324 This is very similar to the biofilm shifts recorded from present-day to high $p\text{CO}_2$ conditions
325 in the Mediterranean Sea (Lidbury et al., 2012; Kerfahi et al., 2014) and in mesocosm
326 conditions (Witt et al., 2011) and suggests a general response of biofilms to increasing CO_2 .

327 Responses to ocean acidification conditions varied between bacterial taxa, some of
328 these increasing whilst others decreased in relative abundance resulting in changes in species
329 richness and diversity (Fig. 1, Fig. 2 and Fig. 3). These findings mirror those of Taylor *et al.*
330 (2014) at CO_2 seeps in Italy, who found that shifts in bacterial biofilm communities involved
331 a similar set of bacterial phyla to those recorded in our study (Fig. 2). Marine
332 bacterioplankton communities also respond to changes in seawater CO_2 with changes in
333 community composition, yet the functions of those communities remain resilient to
334 acidification (Lindh et al., 2013; Lin et al., 2018), as predicted by Joint *et al.* (2011).

335 Holobiont communities can also be affected by ocean acidification conditions. Meron
336 *et al.* (2012) reported shifts in coral bacterial community composition along a pH gradient of
337 8.1-7.3 caused by CO_2 seeps in Italy but found that many taxa were resilient. However,
338 Webster *et al.* (2016) carried out an eight week-long mesocosm experiment and found that
339 coral-associated bacterial taxa were tolerant of elevated $p\text{CO}_2$ (including *Proteobacteria*,
340 *Bacteroidetes*, *Fusobacteria*, *Verrucomicrobia*, *Chloroflexi* and *Planctomycetes*) with no
341 community shifts in these taxa between pH 8.1 ($p\text{CO}_2$ 479–499 μatm) and pH 7.9 ($p\text{CO}_2$
342 738–835 μatm) although they acknowledged that a longer-term experiment might have
343 revealed an effect. In contrast, shifts in hard substratum biofilm microbial community
344 structure were recorded by Webster et al. (2013) who simulated the effects of ocean
345 acidification by bubbling CO_2 into flow-through aquaria and recorded the appearance of new
346 taxa within bacterial biofilm communities as the pH fell. This is similar to the responses we
347 found in relation to pH treatments on Japanese rocky shores, suggesting that perhaps
348 holobiont communities are under tighter control exerted by the host, compared to rocky

349 biofilm communities.

350 It is interesting that there are no major shifts in relative abundance functional groups,
351 for example N fixers and photosynthesizers. Both taxonomic and functional analysis showed
352 that major groups of bacteria (at family and genus levels) remained abundant at the higher
353 pCO₂ levels suggesting that the primary productivity and nutrient cycling of the system did
354 not fundamentally changed, and that most essential biogeochemical functions were still
355 present (Fig. 2) such as the nitrogen fixing activities *Cyanobacteria* and *Chloroflexi*. It is
356 also interesting to note that chemotrophs such as *Halothiobacillus*, *Guyparkeria*,
357 *Thiobacillus*, *Sulfuritortus*, *Nitrosomonas*, *Gallionella* and *Ferriphaeselus* are absent even at
358 the lowest pH treatments. This negative result simultaneously suggests that there may be little
359 change in biogeochemical cycling as a result of such coastal biofilms, and confirms that the
360 CO₂-rich vents are not contaminated with S-containing gases and are indeed pure CO₂ as was
361 originally proposed based on gas and seawater chemistry measurements.

362 However, our conclusions on functional attributes of the biofilms are based only on
363 taxonomic composition and relative abundances. It would be interesting to study the
364 metagenome of these systems as a range of microbial functional processes are thought to be
365 sensitive to ocean pH shifts (Das and Mangwani, 2015).

366 Network analysis revealed that sites having very low pH were more connected than
367 low and ambient pH sites (Fig. 5 and Fig. 6). Network analysis which is based on statistically
368 significant tests of correlation helps to illustrate interactions between taxa, and between
369 particular taxa and particular gene functions (Barberán *et al.*, 2012; Faust and Raes, 2012;
370 Mendes *et al.*, 2014). In networks based on correlation between bacterial OTUs, co-presence
371 associations were stronger than mutual exclusion, implying that most interactions were
372 positive at all studied pH levels, a pattern which is consistent with Lima-Mendez *et al.*,
373 (2015). However, the nearly equal proportions of positive and negative edges demonstrate

374 that taxon-taxon interactions may be regulated by environmental factors. An intact species-
375 rich system would be expected to have greater network complexity due to stable and
376 predictable interactions (Wagg *et al.*, 2014). Our results showed that the sites with very low
377 seawater pH had more complex networks and higher diversity, which indicates that these
378 biofilm communities experienced greater environmental heterogeneity (Lin *et al.*, 2018).
379 *Bacteroidetes* exhibited the most intra-phylum and inter-phylum associations, suggesting that
380 *Bacteroidetes* play crucial roles in the biofilm communities we sampled.

381 Overall, we found that bacterial biofilms had considerable resilience to ocean water
382 acidification, retaining a similar high diversity and functional structure, and stronger network
383 complexity. This contrasts with the simplification of the taxonomic and functional diversity
384 system of larger organisms brought about by decreasing pH in these same coastal systems.
385 Agostini *et al.* (2018) showed that at the acidified sites on both of the habitat types we
386 studied, biofilm and turf algae predominated. The normal succession that occurs on rocky
387 shores had been truncated with simpler and less diverse macrobenthic communities, in line
388 with the findings of Kroeker *et al.* (2013) and Brown *et al.* (2018).

389 There are likely to be multiple mechanisms that drive changes in biofilm bacterial
390 composition along gradients of increasingly acidified conditions. These may include the
391 direct effects of low pH, or low carbonate, or high $p\text{CO}_2$ as well as the indirect effects that
392 occur due to changes in habitat and/or organism interactions. We consider it likely that the
393 bacterial community shifts we observed along pH gradients were partly driven by changes in
394 the broader ecology of the rocky shore system food webs. At our high $p\text{CO}_2$ sites there was a
395 marked reduction in calcified grazers such as littorinid snails, limpets and chitons and an
396 increase in eukaryotic primary producers, such as diatoms (Agostini *et al.*, 2018) all of which
397 would be expected to affect the thickness, extent and composition of biofilm communities.

398 To date, there had been no other studies on the effects of ocean acidification on

399 biofilms in Asia. Our comparison of marine biofilms along a natural pH gradient in Japan
400 supports the view that while there may be pervasive effects of rising $p\text{CO}_2$ levels on marine
401 bacterial biofilm communities, the functional effects may not be major. This warrants further
402 investigation, given that acidification may disrupt biofilm settlement cues for commercially
403 important shellfish, and may affect grazing habitat for a range of marine animals.

404 Our observations contrast with mounting evidence that increasing levels of seawater
405 $p\text{CO}_2$ simplifies marine habitats, maintaining them in an early successional state (Kroeker et
406 al., 2013; Brown et al., 2018). Agostini et al. (2018) showed that biodiverse rocky shore
407 communities (including calcareous macroflora and fauna) were gradually replaced by
408 simpler, less biodiverse communities that are dominated by non-calcified algae and biofilms
409 in areas affected by periods of low carbonate saturation and high dissolved inorganic carbon.
410 Here we showed that at the microbial level bacterial diversity and biofilm connectedness
411 increased, and while communities shifted with unknown effects on biofilm function. Whilst
412 the biofilms will still be fixing and cycling carbon and nutrients, it is possible that a range of
413 other functions (e.g. provision of settlement cues) may be affected. Given the importance of
414 biofilms to coastal ecology, changes in their composition due to globally rising $p\text{CO}_2$ levels
415 requires further investigation to assess the implications for marine ecosystem function.

416

417 **Acknowledgments**

418 We thank Prof. Rich Boden, University of Plymouth, United Kingdom for his suggestions in
419 improving the paper. We also thank Dr. Matthew Chidozie Ogwe, University of Camerino,
420 Italy for his assistance on data analyses and paper editing.

421 **References**

- 422 Agostini, S., Harvey, B. P., Wada, S., Kon, K., Milazzo, M., Inaba, K., et al. (2018). Ocean
423 acidification drives community shifts towards simplified non-calcified habitats in a
424 subtropical-temperate transition zone. *Sci. Rep.* 8, 11354. doi:10.1038/s41598-018-
425 29251-7.
- 426 Azam, F., and Malfatti, F. (2007). Microbial structuring of marine ecosystems. *Nat. Rev.*
427 *Microbiol.* 5, 782. doi:10.1038/nrmicro1747.
- 428 Barberán A, Bates S T, Casamayor E O, Fierer N. 2012. Using network analysis to explore
429 co-occurrence patterns in soil microbial communities. *The ISME journal.* 6: 343.
- 430 Brown, N. E. M., Milazzo, M., Rastrick, S. P. S., Hall-Spencer, J. M., Therriault, T. W., and
431 Harley, C. D. G. (2018). Natural acidification changes the timing and rate of
432 succession, alters community structure, and increases homogeneity in marine
433 biofouling communities. *Glob. Change Biol.* 24, e112–e127. doi:10.1111/gcb.13856.
- 434 Chun, J., Lee, J.-H., Jung, Y., Kim, M., Kim, S., Kim, B. K., et al. (2007). EzTaxon: a web-
435 based tool for the identification of prokaryotes based on 16S ribosomal RNA gene
436 sequences. *Int. J. Syst. Evol. Microbiol.* 57, 2259–2261. doi:10.1099/ijs.0.64915-0.
- 437 Connell, S. D., Kroeker, K. J., Fabricius, K. E., Kline, D. I., and Russell, B. D. (2013). The
438 other ocean acidification problem: CO₂ as a resource among competitors for
439 ecosystem dominance. *Philos. Trans. R. Soc. B Biol. Sci.* 368, 20120442.
440 doi:10.1098/rstb.2012.0442.
- 441 Cornwall, C. E., Revill, A. T., Hall-Spencer, J. M., Milazzo, M., Raven, J. A., and Hurd, C. L.
442 (2017). Inorganic carbon physiology underpins macroalgal responses to elevated CO₂.
443 *Sci. Rep.* 7, 46297. doi:10.1038/srep46297.
- 444 Das, S., and Mangwani, N. (2015). Ocean acidification and marine microorganisms:
445 responses and consequences. *Oceanologia* 57, 349–361.
446 doi:10.1016/j.oceano.2015.07.003.
- 447 de Carvalho, C. C. (2018). Marine biofilms: A successful microbial strategy with economic
448 implications. *Front. Mar. Sci.* 5, 126. doi:10.3389/fmars.2018.00126.
- 449 Decho, A. W. (2000). Microbial biofilms in intertidal systems: an overview. *Cont. Shelf Res.*
450 20, 1257–1273. doi:10.1016/S0278-4343(00)00022-4.
- 451 Dickson, A. G. (1990). Thermodynamics of the dissociation of boric acid in potassium
452 chloride solutions from 273.15 to 318.15 K. *J. Chem. Eng. Data* 35, 253–257.
453 doi:10.1021/je00061a009.
- 454 Dickson, A. G., and Millero, F. J. (1987). A comparison of the equilibrium constants for the
455 dissociation of carbonic acid in seawater media. *Deep Sea Res. Part Oceanogr. Res.*
456 *Pap.* 34, 1733–1743. doi:10.1016/0198-0149(87)90021-5.
- 457 Dong, K., Tripathi, B., Moroenyane, I., Kim, W., Li, N., Chu, H., et al. (2016). Soil fungal
458 community development in a high Arctic glacier foreland follows a directional
459 replacement model, with a mid-successional diversity maximum. *Sci. Rep.* 6, 26360.

- 460 doi:10.1038/srep26360.
- 461 Edgar, R. C., Haas, B. J., Clemente, J. C., Quince, C., and Knight, R. (2011). UCHIME
462 improves sensitivity and speed of chimera detection. *Bioinformatics* 27, 2194–2200.
463 doi:10.1093/bioinformatics/btr381.
- 464 Fabricius, K. E., Langdon, C., Uthicke, S., Humphrey, C., Noonan, S., De'ath, G., et al.
465 (2011). Losers and winners in coral reefs acclimatized to elevated carbon dioxide
466 concentrations. *Nat. Clim. Change* 1, 165–169. doi:10.1038/nclimate1122.
- 467 Faust K, Raes J. 2012. Microbial interactions: From networks to models. *Nature Reviews*
468 *Microbiology*. **10**: 538-550.
- 469 Hall-Spencer, J. M., Rodolfo-Metalpa, R., Martin, S., Ransome, E., Fine, M., Turner, S. M.,
470 et al. (2008). Volcanic carbon dioxide vents show ecosystem effects of ocean
471 acidification. *Nature* 454, 96–99. doi:10.1038/nature07051.
- 472 Hassenrück, C., Hofmann, L. C., Bischof, K., and Ramette, A. (2015). Seagrass biofilm
473 communities at a naturally CO₂-rich vent. *Environ. Microbiol. Rep.* 7, 516–525.
474 doi:10.1111/1758-2229.12282.
- 475 Hassenrück, C., Tegetmeyer, H. E., Ramette, A., Fabricius, K. E., and Handling editor:
476 Woodson CB (2017). Minor impacts of reduced pH on bacterial biofilms on
477 settlement tiles along natural pH gradients at two CO₂ seeps in Papua New Guinea.
478 *ICES J. Mar. Sci.* 74, 978–987. doi:10.1093/icesjms/fsw204.
- 479 Huse, S. M., Welch, D. M., Morrison, H. G., and Sogin, M. L. (2010). Ironing out the
480 wrinkles in the rare biosphere through improved OTU clustering. *Environ. Microbiol.*
481 12, 1889–1898. doi:10.1111/j.1462-2920.2010.02193.x.
- 482 Johnson, R. V., Brownlee, C., Milazzo, M., and Hall-Spencer, M. J. (2015). Marine
483 microphytobenthic assemblage shift along a natural shallow-water CO₂ gradient
484 subjected to multiple environmental stressors. *J. Mar. Sci. Eng.* 3.
485 doi:10.3390/jmse3041425.
- 486 Joint, I., Doney, S. C., and Karl, D. M. (2011). Will ocean acidification affect marine
487 microbes? *ISME J.* 5, 1. doi:10.1038/ismej.2010.79.
- 488 Kerfahi, D., Hall-Spencer, J. M., Tripathi, B. M., Milazzo, M., Lee, J., and Adams, J. M.
489 (2014). Shallow water marine sediment bacterial community shifts along a natural
490 CO₂ gradient in the Mediterranean Sea off Vulcano, Italy. *Microb. Ecol.* 67, 819–828.
491 doi:10.1007/s00248-014-0368-7.
- 492 Krause, E., Wichels, A., Giménez, L., Lunau, M., Schilhabel, M. B., and Gerdtts, G. (2012).
493 Small changes in pH have direct effects on marine bacterial community composition:
494 a microcosm approach. *PLoS One* 7, e47035. doi:10.1371/journal.pone.0047035.
- 495 Kroeker, K. J., Gambi, M. C., and Micheli, F. (2013). Community dynamics and ecosystem
496 simplification in a high-CO₂ ocean. *Proc. Natl. Acad. Sci. U. S. A.* 110, 12721–12726.
497 doi:10.1073/pnas.1216464110.
- 498 Lau, S. C., Thiyagarajan, V., Cheung, S. C., and Qian, P.-Y. (2005). Roles of bacterial

- 499 community composition in biofilms as a mediator for larval settlement of three
500 marine invertebrates. *Aquat. Microb. Ecol.* 38, 41–51. doi:10.3354/ame038041.
- 501 Lauber, C. L., Strickland, M. S., Bradford, M. A., and Fierer, N. (2008). The influence of soil
502 properties on the structure of bacterial and fungal communities across land-use types.
503 *Soil Biol. Biochem.* 40, 2407–2415. doi:10.1016/j.soilbio.2008.05.021.
- 504 Lewis, J. R. (1964). *The Ecology of Rocky Shores*. London, UK: English Universities Press.
- 505 Lidbury, I., Johnson, V., Hall-Spencer, J. M., Munn, C. B., and Cunliffe, M. (2012).
506 Community-level response of coastal microbial biofilms to ocean acidification in a
507 natural carbon dioxide vent ecosystem. *Mar. Pollut. Bull.* 64, 1063–1066.
508 doi:10.1016/j.marpolbul.2012.02.011.
- 509 Lima-Mendez G, Faust K, Henry N, Decelle J, Colin S, Carcillo F, Chaffron S, Ignacio-
510 Espinosa J C, Roux S, Vincent F. 2015. Determinants of community structure in the
511 global plankton interactome. *Science*. **348**: 1262073.
- 512 Lin, X., Huang, R., Li, Y., Li, F., Wu, Y., Hutchins, D. A., et al. (2018). Interactive network
513 configuration maintains bacterioplankton community structure under elevated CO₂ in
514 a eutrophic coastal mesocosm experiment. *Biogeosciences* 15, 551–565.
515 doi:10.5194/bg-15-551-2018.
- 516 Lindh, M. V., Riemann, L., Baltar, F., Romero-Oliva, C., Salomon, P. S., Granéli, E., et al.
517 (2013). Consequences of increased temperature and acidification on bacterioplankton
518 community composition during a mesocosm spring bloom in the Baltic Sea. *Environ.*
519 *Microbiol. Rep.* 5, 252–262. doi:10.1111/1758-2229.12009.
- 520 Liu, J., Weinbauer, M. G., Maier, C., Dai, M., and Gattuso, J. P. (2010). Effect of ocean
521 acidification on microbial diversity and on microbe-driven biogeochemistry and
522 ecosystem functioning. *Aquat. Microb. Ecol.* 61, 291–305. doi:10.3354/ame01446.
- 523 Mehrbach, C., Culberson, C. H., Hawley, J. E., and Pytkowicz, R. M. (1973). Measurement
524 of the apparent dissociation constants of carbonic acid in seawater at atmospheric
525 pressure. *Limnol. Oceanogr.* 18, 897–907. doi:10.4319/lo.1973.18.6.0897.
- 526 Mendes L W, Kuramae E E, Navarrete A A, Van Veen J A, Tsai S M. 2014. Taxonomical and
527 functional microbial community selection in soybean rhizosphere. *The ISME journal*.
528 **8**: 1577-1587.
- 529 Meron, D., Rodolfo-Metalpa, R., Cunning, R., Baker, A. C., Fine, M., and Banin, E. (2012).
530 Changes in coral microbial communities in response to a natural pH gradient. *ISME J.*
531 **6**, 1775. doi:10.1038/ismej.2012.19.
- 532 Meyer, F., Paarmann, D., D’Souza, M., Olson, R., Glass, E. M., Kubal, M., et al. (2008). The
533 metagenomics RAST server—a public resource for the automatic phylogenetic and
534 functional analysis of metagenomes. *BMC Bioinformatics* 9, 386. doi:10.1186/1471-
535 2105-9-386.
- 536 Morrow, K. M., Bourne, D. G., Humphrey, C., Botté, E. S., Laffy, P., Zaneveld, J., et al.
537 (2014). Natural volcanic CO₂ seeps reveal future trajectories for host–microbial
538 associations in corals and sponges. *Isme J.* 9, 894. doi:10.1038/ismej.2014.188.

- 539 O'Brien, P. A., Smith, H. A., Fallon, S., Fabricius, K., Willis, B. L., Morrow, K. M., et al.
540 (2018). Elevated CO₂ has little influence on the bacterial communities associated with
541 the pH-tolerant coral, massive *Porites* spp. *Front. Microbiol.* 9, 2621.
542 doi:10.3389/fmicb.2018.02621.
- 543 Oksanen, J., Kindt, R., Legendre, P., O'Hara, B., Simpson, G. L., Solymos, P., et al. (2008).
544 The vegan package. *Community Ecol. Packag.-Forge R-Proj. Orgprojectsvegan*.
- 545 Pierrot, D., Lewis, E., and Wallace, D. W. R. (2006). *MS Excel Program Developed for CO₂*
546 *System Calculations, ORNL/CDIAC-105*. Oak Ridge, Tennessee.
- 547 Porzio, L., Buia, M. C., and Hall-Spencer, J. M. (2011). Effects of ocean acidification on
548 macroalgal communities. *J. Exp. Mar. Biol. Ecol.* 400, 278–287.
549 doi:10.1016/j.jembe.2011.02.011.
- 550 Qian, P.-Y., Lau, S. C., Dahms, H.-U., Dobretsov, S., and Harder, T. (2007). Marine biofilms
551 as mediators of colonization by marine macroorganisms: implications for antifouling
552 and aquaculture. *Mar. Biotechnol.* 9, 399–410. doi:10.1007/s10126-007-9001-9.
- 553 Rastrick, S. S. P., Graham, H., Azetsu-Scott, K., Calosi, P., Chierici, M., Fransson, A., et al.
554 (2018). Using natural analogues to investigate the effects of climate change and ocean
555 acidification on Northern ecosystems. *ICES J. Mar. Sci.*, fsy128–fsy128.
556 doi:10.1093/icesjms/fsy128.
- 557 Riebesell, U., and Gattuso, J.-P. (2015). Lessons learned from ocean acidification research.
558 *Nat. Clim. Change* 5, 12–14. doi:10.1038/nclimate2456.
- 559 Rodríguez-Gironés, M. A., and Santamaría, L. (2006). A new algorithm to calculate the
560 nestedness temperature of presence–absence matrices. *J. Biogeogr.* 33, 924–935.
561 doi:10.1111/j.1365-2699.2006.01444.x.
- 562 Schloss, P. D., Westcott, S. L., Ryabin, T., Hall, J. R., Hartmann, M., Hollister, E. B., et al.
563 (2009). Introducing mothur: open-source, platform-independent, community-
564 supported software for describing and comparing microbial communities. *Appl.*
565 *Environ. Microbiol.* 75, 7537–7541. doi:10.1128/AEM.01541-09.
- 566 Sunday, J. M., Fabricius, K. E., Kroeker, K. J., Anderson, K. M., E, B. N., Barry, J. P., et al.
567 (2017). Ocean acidification can mediate biodiversity shifts by changing biogenic
568 habitat. *Nat. Clim. Change* 7, 81–85. doi:10.1038/nclimate3161.
- 569 Taylor, J. D., Ellis, R., Milazzo, M., Hall-Spencer, J. M., and Cunliffe, M. (2014). Intertidal
570 epilithic bacteria diversity changes along a naturally occurring carbon dioxide and pH
571 gradient. *FEMS Microbiol. Ecol.* 89, 670–678. doi:10.1111/1574-6941.12368.
- 572 Thompson, R., Norton, T., and Hawkins, S. (2004). Physical stress and biological control
573 regulate the producer–consumer balance in intertidal biofilms. *Ecology* 85, 1372–
574 1382. doi:10.1890/03-0279.
- 575 Tolker-Nielsen, T., and Molin, S. (2000). Spatial organization of microbial biofilm
576 communities. *Microb. Ecol.* 40, 75–84. doi:10.1007/s002480000057.
- 577 Tripathi, B. M., Kim, M., Singh, D., Lee-Cruz, L., Lai-Hoe, A., Ainuddin, A., et al. (2012).

578 Tropical soil bacterial communities in Malaysia: pH dominates in the equatorial
579 tropics too. *Microb. Ecol.* 64, 474–484. doi:10.1007/s00248-012-0028-8.

580 Uppström, L. R. (1974). The boron/chlorinity ratio of deep-sea water from the Pacific Ocean.
581 *Deep Sea Res. Oceanogr. Abstr.* 21, 161–162. doi:10.1016/0011-7471(74)90074-6.

582 Wagg C, Bender S F, Widmer F, van der Heijden M G. 2014. Soil biodiversity and soil
583 community composition determine ecosystem multifunctionality. *Proceedings of the*
584 *National Academy of Sciences.* **111**: 5266-5270.

585 Webster, N., Negri, A., Botté, E., Laffy, P., Flores, F., Noonan, S., et al. (2016). Host-
586 associated coral reef microbes respond to the cumulative pressures of ocean warming
587 and ocean acidification. *Sci. Rep.* 6, 19324. doi:10.1038/srep19324.

588 Webster, N., Negri, A., Flores, F., Humphrey, C., Soo, R., Botte, E., et al. (2013). Near-future
589 ocean acidification causes differences in microbial associations within diverse coral
590 reef taxa. *Environ. Microbiol. Rep.* 5, 243–251. doi:10.1111/1758-2229.12006.

591 Weinbauer, M. G., Mari, X., and Gattuso, J.-P. (2011). “Effect of ocean acidification on the
592 diversity and activity of heterotrophic marine microorganisms,” in *Ocean*
593 *Acidification* (Oxford, UK: Oxford University Press), 83–98.

594 Williams, G. A., Davies, M. S., and Nagarkar, S. (2000). Primary succession on a seasonal
595 tropical rocky shore: the relative roles of spatial heterogeneity and herbivory. *Mar.*
596 *Ecol. Prog. Ser.* 203, 81–94. doi:10.3354/meps203081.

597 Witt, V., Wild, C., Anthony, K. R. N., Diaz-Pulido, G., and Uthicke, S. (2011). Effects of
598 ocean acidification on microbial community composition of, and oxygen fluxes
599 through, biofilms from the Great Barrier Reef. *Environ. Microbiol.* 13, 2976–2989.
600 doi:10.1111/j.1462-2920.2011.02571.x.

601 Wootton, J. T., Pfister, C. A., and Forester, J. D. (2008). Dynamic patterns and ecological
602 impacts of declining ocean pH in a high-resolution multi-year dataset. *Proc. Natl.*
603 *Acad. Sci. U. S. A.* 105, 18848–18853. doi:10.1073/pnas.0810079105.

604 Yachi, S., and Loreau, M. (1999). Biodiversity and ecosystem productivity in a fluctuating
605 environment: the insurance hypothesis. *Proc. Natl. Acad. Sci. U. S. A.* 96, 1463–1468.
606 doi:10.1073/pnas.96.4.1463.

607

608

Table legends

Table 1. Sea water chemistry across different sampling sites along pH gradient.

Table 2. Results of multivariate PERMANOVA showing significant differences in biofilm bacterial community composition between different sites along pH gradient.

Figure legends

Fig. 1. Biofilm bacterial alpha-diversity (mean \pm SE) at different seawater pH levels in Shikine Island, Japan. Variation of OTUs richness in **(a)** boulder sites and **(b)** cliff sites. And variation of Shannon index **(c)** boulder sites and **(d)** cliff sites.

Fig. 2. Relative abundance of biofilm bacterial phyla detected along a pH gradient in Shikine Island, Japan.

Fig. 3. Relative abundance of biofilm bacterial taxa detected along a pH gradient in Shikine Island, Japan at **(a)** order level and **(b)** family level.

Fig. 4. NMDS ordination of total bacterial community composition among **(a)** different pH levels and **(b)** habitat types, based on Bray-Curtis distance.

Fig. 5. Frequency of co-occurrence patterns of sampled sites along a pH gradient in Shikine Island, Japan.

Fig. 6. Number of inter-Phylum and intra-Phylum co-presences and mutual exclusions of sampled sites (A: very low cliff site; B: low cliff site; C: ambient cliff site; D: very low boulder site; E: low boulder site; F: ambient boulder site).

Fig. 7. Box plot representing the relative abundance of the (a) Methane metabolism, (b) Sulphur metabolism, (c) Nitrogen metabolism, (d) Energy metabolism, (e) Carbon fixation in Prokaryotes and (f) Carbon fixation in photosynthetic organisms. The analysis was based on KEGG module

predictions using 16S data with the software PICRUSt. Results from multiple group comparisons in function abundance (ANOVA, Tukey–Kramer, $P < 0.05$) is reported as corrected P -value (Storey’s FDR multiple test correction approach). The median value is shown as a line within the box and the mean value as a star. Error bars represent standard deviations.

Supplementary Online Material

Table S1. Results from two-way ANOVA showing the variation of the relative abundance of biofilm bacterial phyla across different sites.

Table S2. Results from two-way ANOVA showing the variation of the relative abundance of biofilm bacterial orders across different sites.

Table S3. Results from two-way ANOVA showing the variation of the relative abundance of biofilm bacterial families across different sites.

Table S4. Samples of “Boulder-Very low” and “Cliff-Ambient” sites formed the lowest nest while the other samples are basically a subset of these.

Fig. S1. Location of sample sites off Shikine Island, Japan.

Fig. S2. Rock biofilm sampling along a pH gradient off Shikine Island, Japan.

Fig. S3. Rarefaction curves comparing rock biofilm bacterial communities along a seawater pH gradient off Shikine Island, Japan.

Fig. S4. Predicted differences in biofilm bacterial functional categories (PICRUSt) across boulder and cliff sites off Shikine Island, Japan.

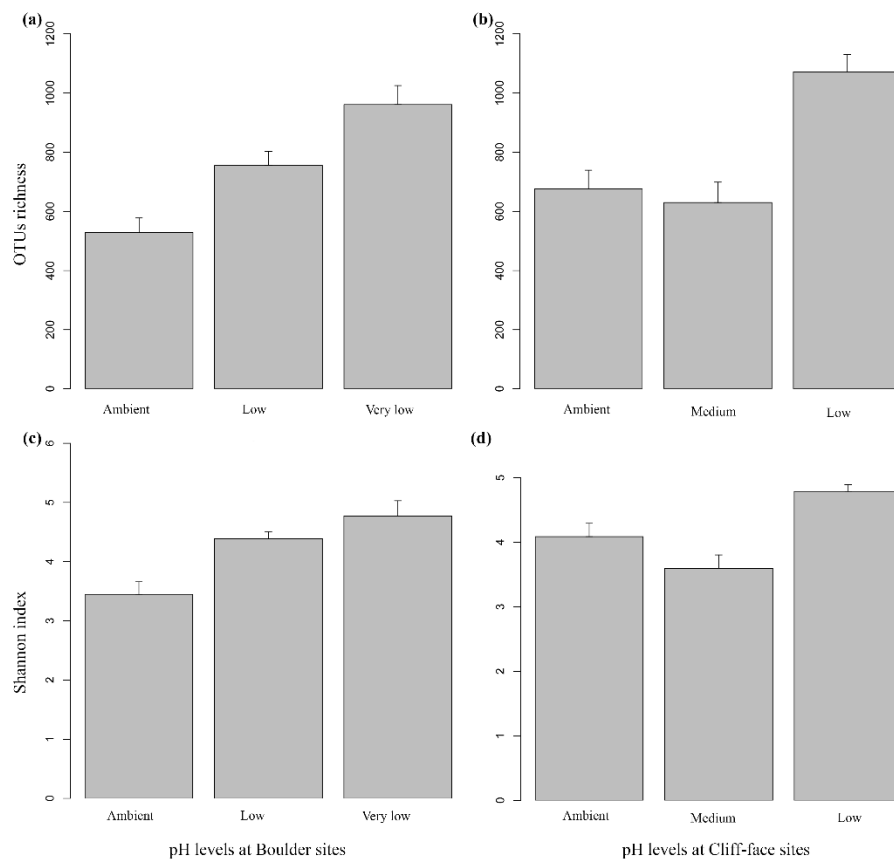


Fig. 1. Biofilm bacterial alpha-diversity (mean \pm SE) at different seawater pH levels in Shikine Island, Japan. Variation of OTUs richness in (a) boulder sites and (b) cliff sites. And variation of Shannon index (c) boulder sites and (d) cliff sites.

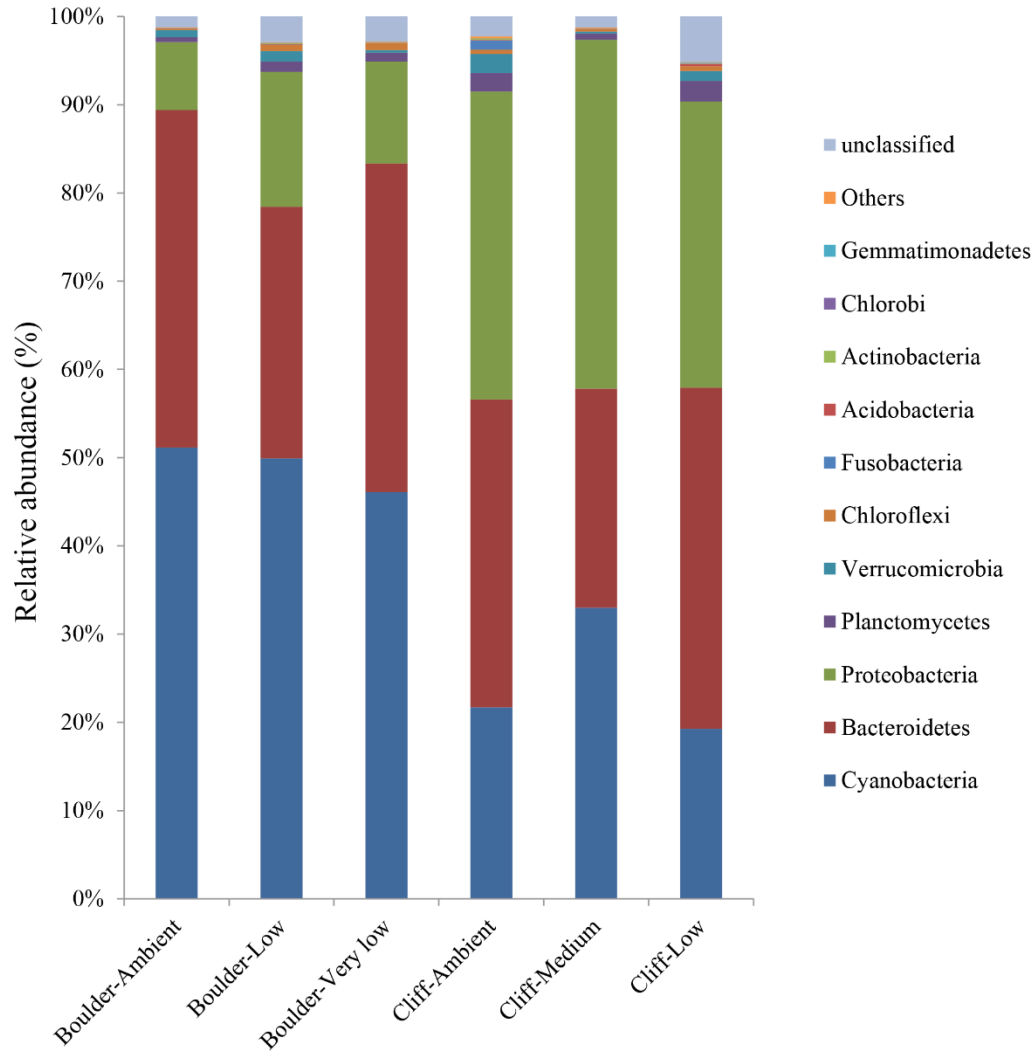


Fig. 2. Relative abundance of biofilm bacterial phyla detected along different sites in Shikine Island, Japan.

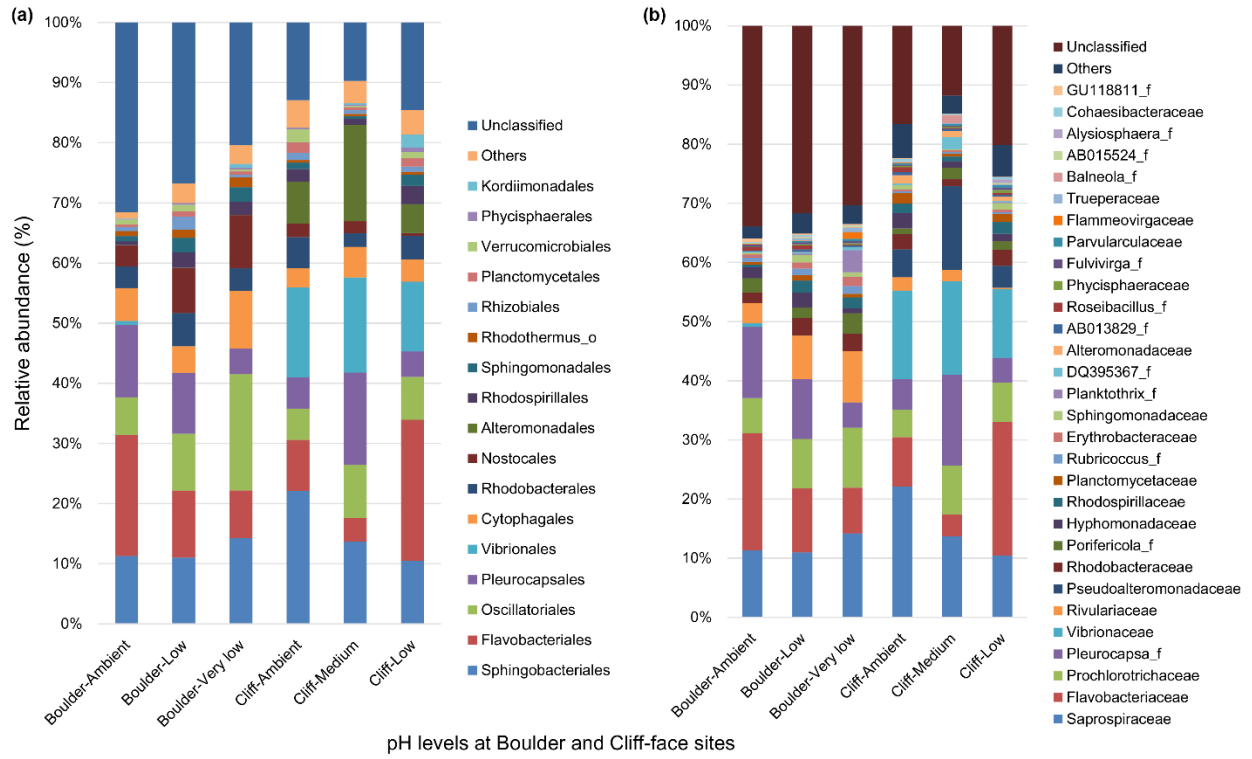


Fig. 3. Relative abundance of biofilm bacterial taxa detected along a pH gradient in Shikine Island, Japan at **a)** order level and **b)** family level.

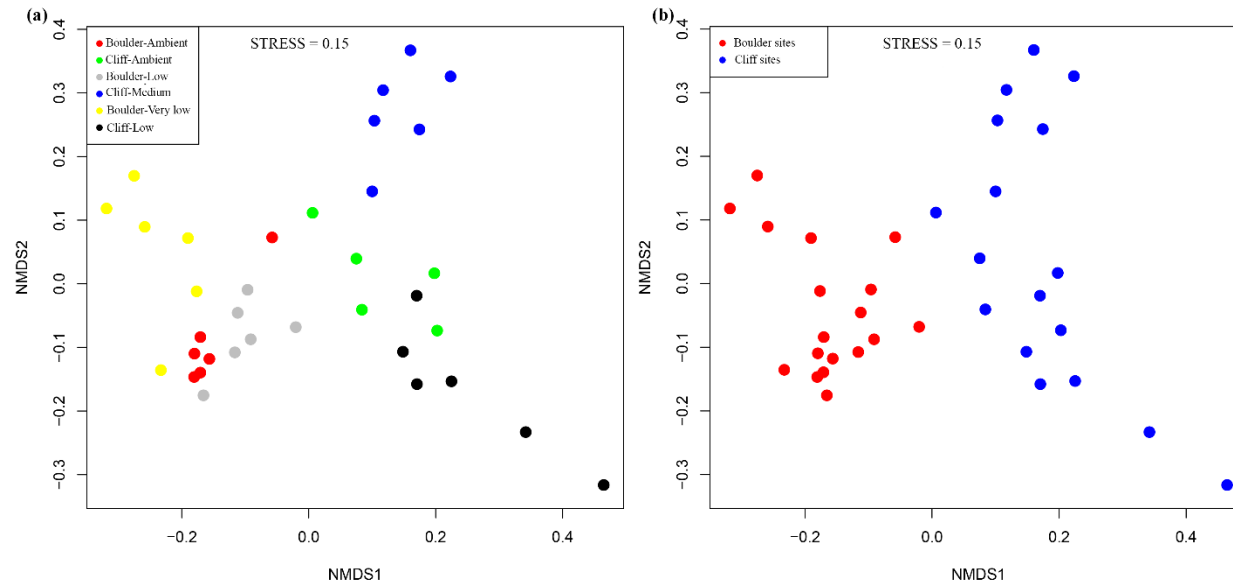


Fig. 4. NMDS ordination of total bacterial community composition among (a) different pH levels and (b) habitat types, based on Bray-Curtis distance.

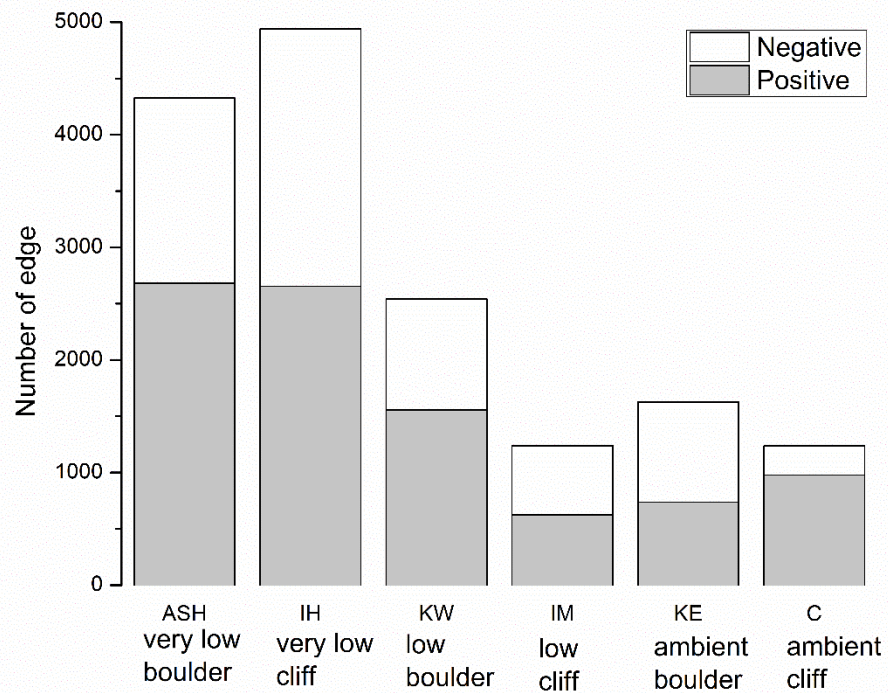


Fig. 5. Frequency of co-occurrence patterns of sampled stations.

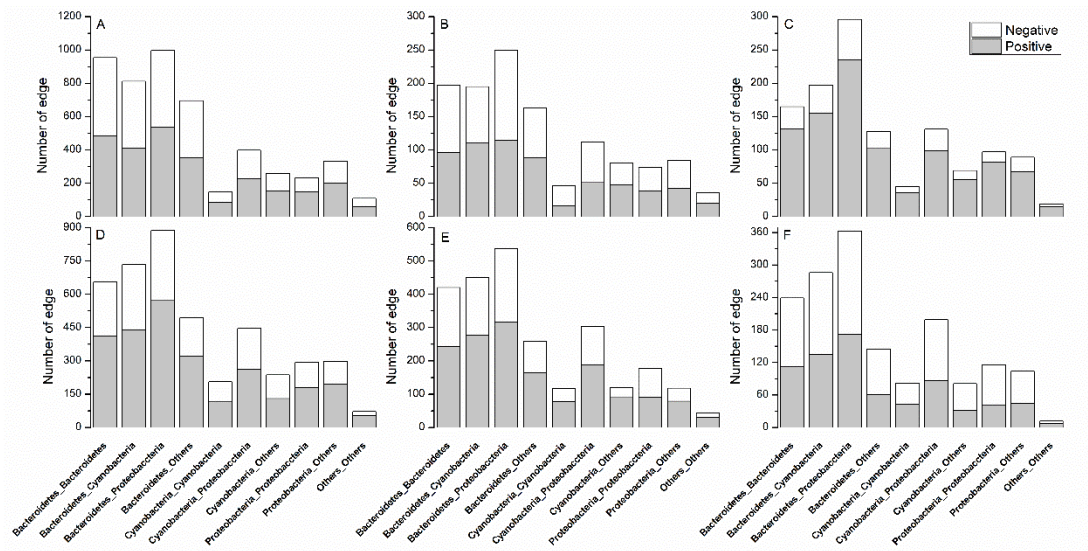


Fig. 6. Number of inter-Phylum and intra-Phylum co-presences and mutual exclusions of sampled stations (A: IH; B: IM; C: C; D: ASH; D: KW; F: KE).

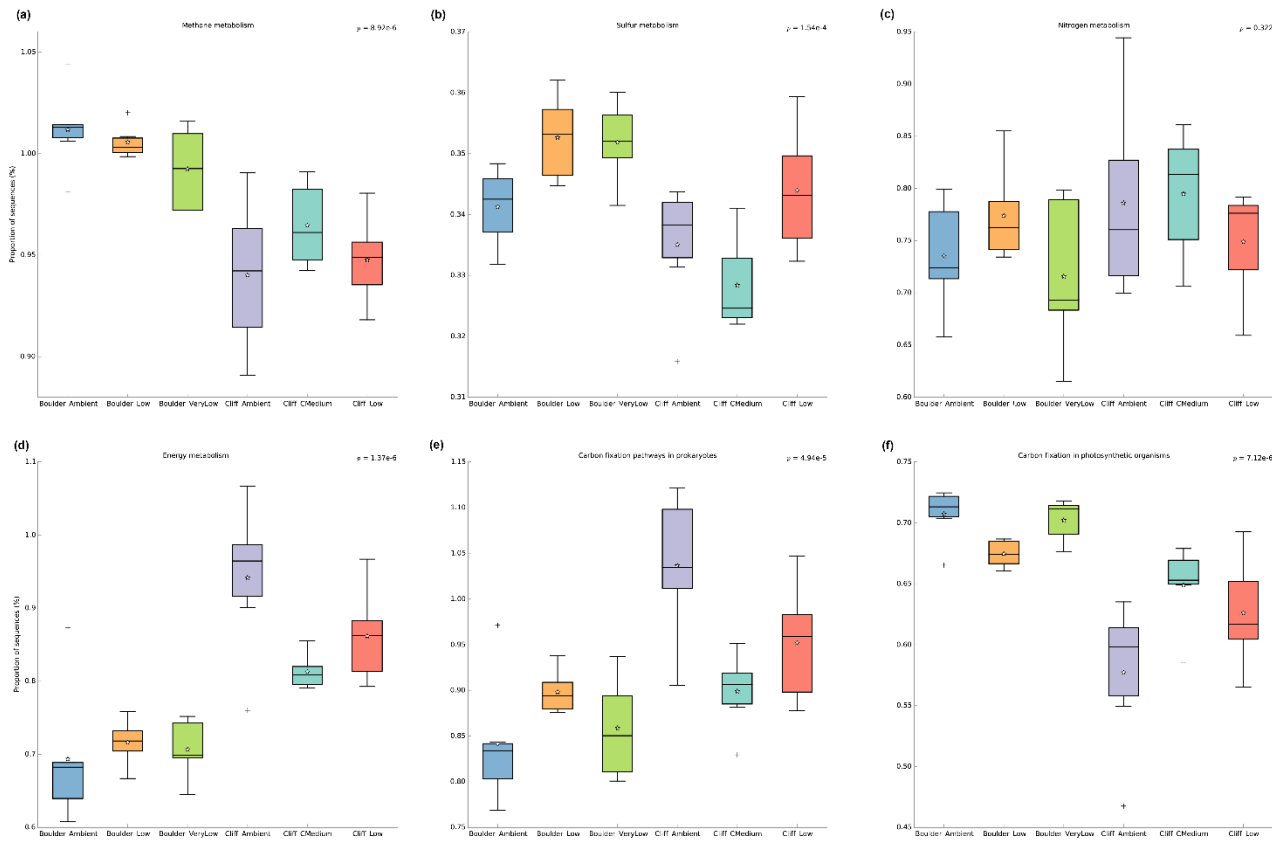


Fig. 7. Box plot representing the relative abundance of the (a) Methane metabolism, (b) Sulphur metabolism, (c) Nitrogen metabolism, (d) Energy metabolism, (e) Carbon fixation in Prokaryotes and (f) Carbon fixation in photosynthetic organisms. The analysis was based on KEGG module predictions using 16S data with the software PICRUSt. Results from multiple group comparisons in function abundance (ANOVA, Tukey–Kramer, $P < 0.05$) is reported as corrected P -value (Storey’s FDR multiple test correction approach). The median value is shown as a line within the box and the mean value as a star. Error bars represent standard deviations.

Table 1. Sea water chemistry across different sampling sites along pH gradient.

Habitat type	pH zone	Salinity (psu)	Temp (°C)	A _T (μmol kg ⁻¹)	DIC (μmol kg ⁻¹)	pH _{NBS}	pCO ₂ (matm)	HCO ₃ ⁻ (μmol kg ⁻¹)	CO ₃ ²⁻ (μmol kg ⁻¹)	Ω _{Ca}	Ω _{Ar}
Boulder	Ambient	34.0 ± 0.1	20.5 ± 0.7	2241.7 ± 12.5	1930.3 ± 20.6	8.28 ± 0.03	290.6 ± 25.1	1702.7 ± 33.1	218.3 ± 13.4	5.26 ± 0.32	3.42 ± 0.21
Boulder	Low	34.0 ± 0.2	20.4 ± 0.7	2201.4 ± 57.0	2141.5 ± 23.9	7.70 ± 0.07	1320.6 ± 225.4	2029.7 ± 27.9	69.4 ± 11.3	1.67 ± 0.27	1.09 ± 0.18
Boulder	Very low	34.1 ± 0.1	20.5 ± 0.5	2162.7 ± 31.7	2253.7 ± 37.6	7.24 ± 0.10	4003.9 ± 877	2100.2 ± 16.0	25.2 ± 6.5	0.61 ± 0.16	0.40 ± 0.10
Cliff	Ambient	34.0 ± 0.0	19.4 ± 0.5	2237.4 ± 1.0	1938.9 ± 36.3	8.27 ± 0.06	298.6 ± 51	1719.6 ± 58.1	209.4 ± 23.5	5.04 ± 0.57	3.27 ± 0.37
Cliff	Medium	34.0 ± 0.1	17.5 ± 1.1	2249.7 ± 2.1	2028.1 ± 35.9	8.15 ± 0.07	419.2 ± 82.3	1853.0 ± 55.1	160.5 ± 22.4	3.86 ± 0.54	2.49 ± 0.35
Cliff	Low	34.0 ± 0.0	18.5 ± 0.7	2281.7 ± 31.3	2186.8 ± 82.4	7.81 ± 0.22	1181.5 ± 672.4	2054.4 ± 103.6	92.3 ± 42.1	2.22 ± 1.01	1.44 ± 0.66

Supplementary Online Material

Responses of intertidal bacterial biofilm communities to increasing $p\text{CO}_2$ in a naturally acidified system

Dorsaf Kerfahi¹, Ben Harvey², Sylvain Agostini², Koetsu Kon², Ruiping Huang³, Jonathan M. Adams^{4*}, Jason M. Hall-Spencer^{2,5}

¹School of Applied Biosciences, College of Agriculture and Life Sciences, Kyungpook National University, Daegu, 41566, Republic of Korea.

²Shimoda Marine Research Center, University of Tsukuba, 5-10-1 Shimoda, Shizuoka, Japan.

³State Key Laboratory of Marine Environmental Science, Xiamen University, Xiamen, Fujian, 361100, China.

⁴School of Geographic and Oceanographic Sciences, Nanjing University, Nanjing 210008, China.

⁵School of Biological and Marine Sciences, University of Plymouth, Plymouth, PL4 8AA, United Kingdom.

***Corresponding author:** Jonathan M. Adams.

School of Geographic and Oceanographic Sciences, Nanjing University, Nanjing 210008, China.

E-mail: foundinkualalumpur@yahoo.com

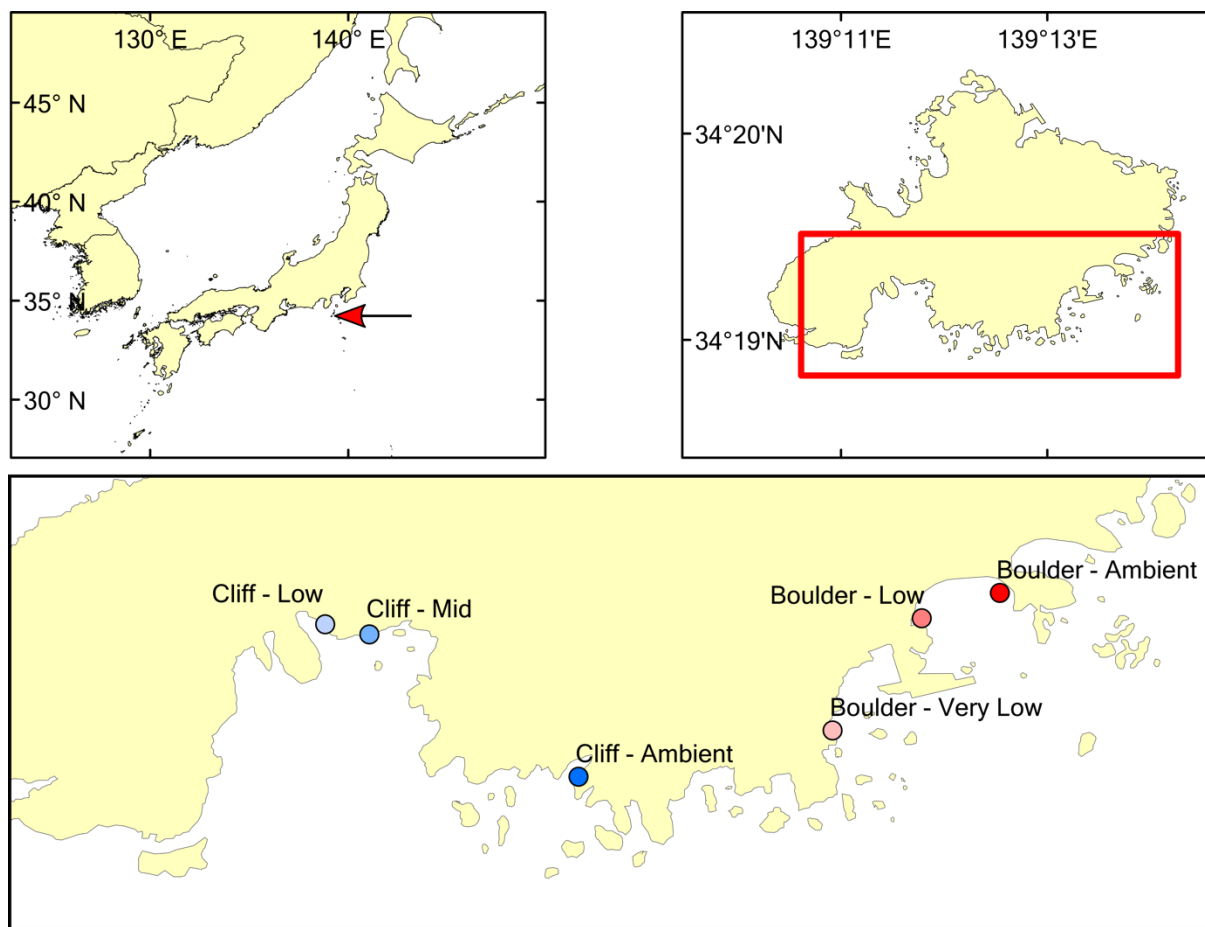


Fig. S1. Location of sample sites off Shikine Island, Japan.



Fig. S2. Rock biofilm sampling along a pH gradient off Shikine Island, Japan.

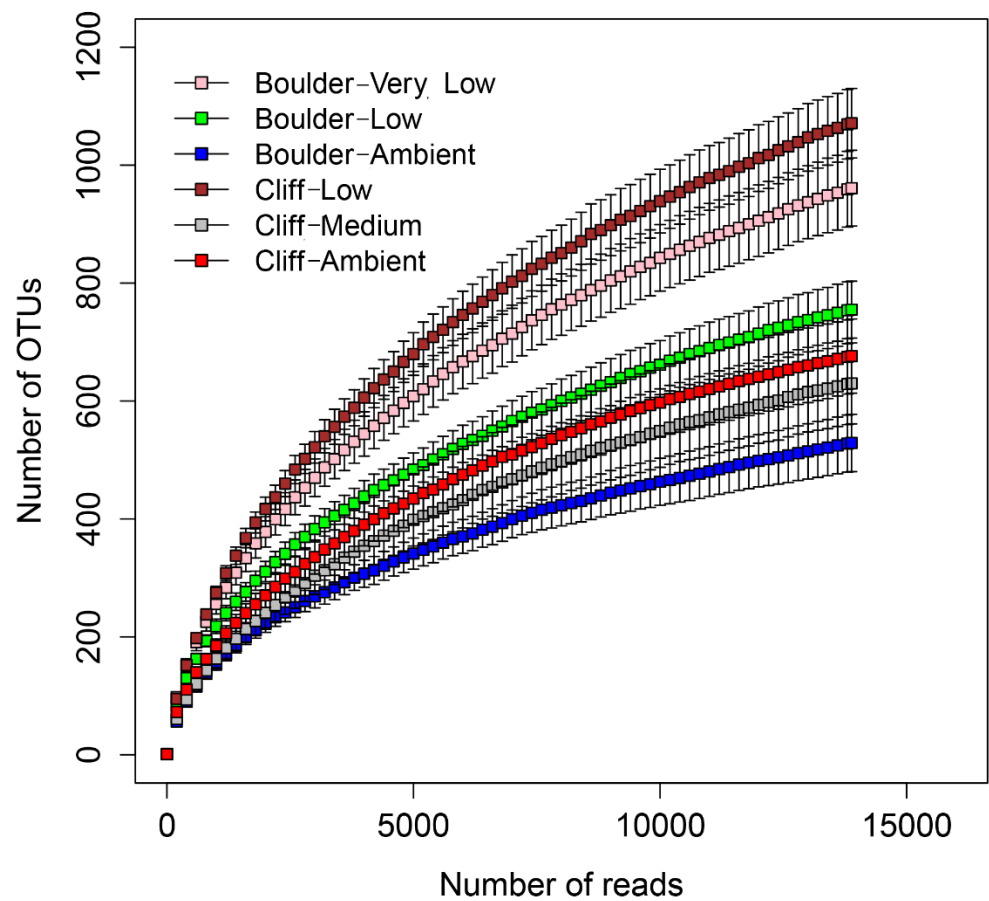
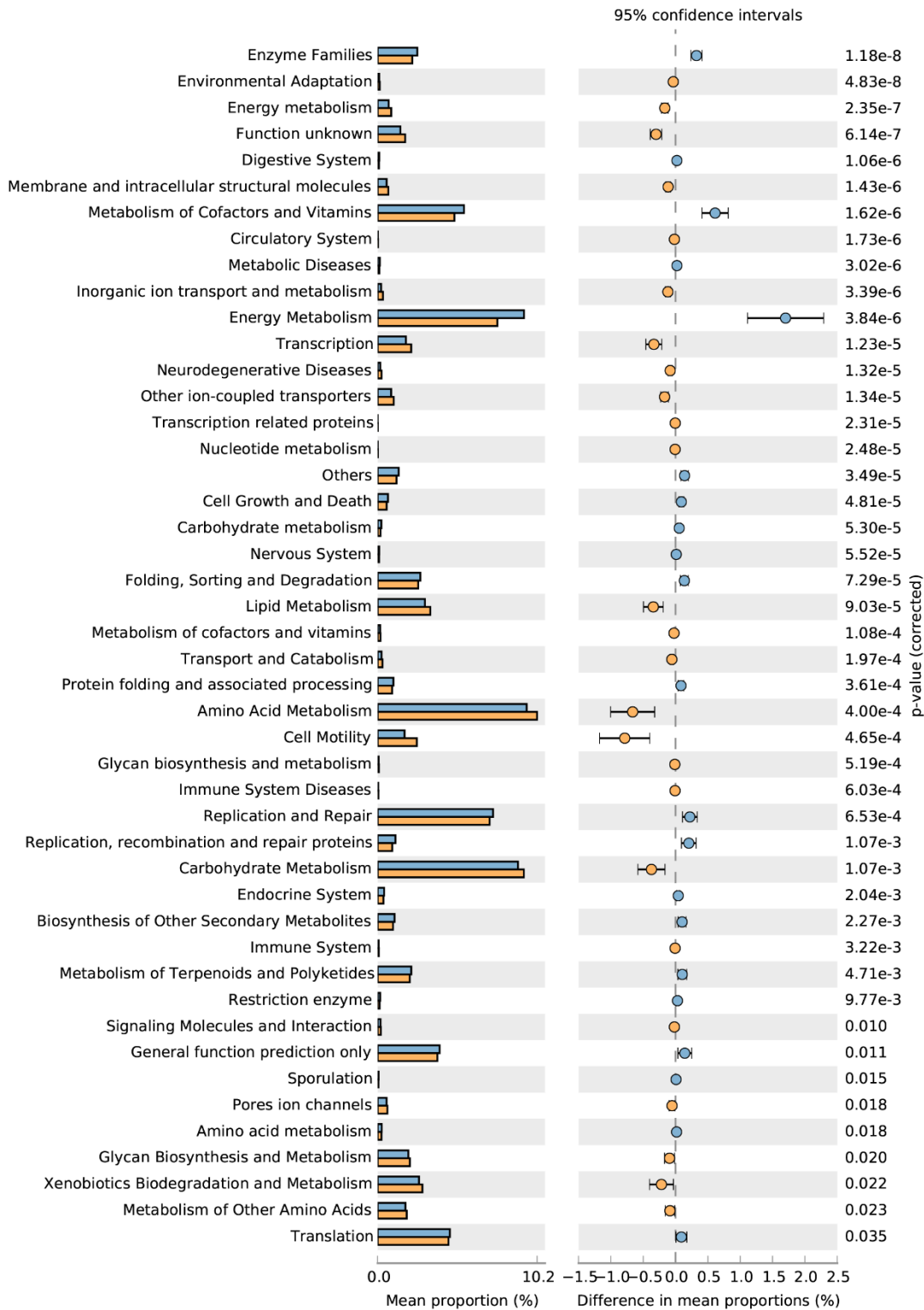


Fig. S3. Rarefaction curves comparing rock biofilm bacterial communities along a seawater pH gradient off Shikine Island, Japan.



1

2 **Fig. S4.** Predicted differences in biofilm bacterial functional categories (PICRUST) across
 3 boulder and cliff sites off Shikine Island, Japan.

4

Supplementary Online Material

5 **Responses of intertidal bacterial biofilm communities to increasing $p\text{CO}_2$ in**
6 **a naturally acidified system**

7 Dorsaf Kerfahi¹, Ben Harvey², Sylvain Agostini², Koetsu Kon², Ruiping Huang³, Jonathan M.
8 Adams^{4*}, Jason M. Hall-Spencer^{2,5}

9

10 ¹School of Applied Biosciences, College of Agriculture and Life Sciences, Kyungpook
11 National University, Daegu, 41566, Republic of Korea.

12 ²Shimoda Marine Research Center, University of Tsukuba, 5-10-1 Shimoda, Shizuoka, Japan.

13 ³State Key Laboratory of Marine Environmental Science, Xiamen University, Xiamen,
14 Fujian, 361100, China.

15 ⁴School of Geographic and Oceanographic Sciences, Nanjing University, Nanjing 210008,
16 China.

17 ⁵School of Biological and Marine Sciences, University of Plymouth, Plymouth, PL4 8AA,
18 United Kingdom.

19

20 ***Corresponding author:** Jonathan M. Adams.

21 School of Geographic and Oceanographic Sciences, Nanjing University, Nanjing 210008,
22 China.

23 E-mail: foundinkualalumpur@yahoo.com

Table S1. Results from two-way ANOVA showing the variation of the relative abundance of biofilm bacterial phyla across different sites.

		df	Mean square	F model	P value
Cyanobacteria	Habitat type	1	5279	67.76	<0.001
	pH	2	234	3	0.064
	Habitat type * pH	2	133	1.7	0.19
Bacteroidetes	Habitat type	1	28.8	0.31	0.58
	pH	2	451	4.85	0.01
	Habitat type * pH	2	26.4	0.28	0.75
Proteobacteria	Habitat type	1	5229	38.33	<0.001
	pH	2	134	0.98	0.38
	Habitat type * pH	2	29	0.21	0.8
Planctomycetes	Habitat type	1	5.81	12.48	0.001
	pH	2	1.52	3.27	0.05
	Habitat type * pH	2	3.67	7.9	0.001
Verrucomicrobia	Habitat type	1	1.5	1.58	0.21
	pH	2	2.49	2.68	0.08
	Habitat type * pH	2	4.38	4.61	0.01
Chloroflexi	Habitat type	1	0.08	0.45	0.5
	pH	2	0.38	2.09	0.14
	Habitat type * pH	2	0.44	2.43	0.1
Fusobacteria	Habitat type	1	1.04	0.96	0.33
	pH	2	1.11	1.02	0.37
	Habitat type * pH	2	1.06	0.97	0.38
Acidobacteria	Habitat type	1	0.03	2.93	0.09
	pH	2	0.02	1.72	0.19
	Habitat type * pH	2	0.05	3.71	0.03
Actinobacteria	Habitat type	1	0.0004	0.07	0.79
	pH	2	0.009	1.47	0.24
	Habitat type * pH	2	0.02	4.48	0.01
Chlorobi	Habitat type	1	0.00005	0.02	0.8
	pH	2	0.006	3.02	0.06
	Habitat type * pH	2	0.001	0.52	0.59
Gemmatimonadetes	Habitat type	1	0.001	2.58	0.11
	pH	2	0.0009	1.7	0.19
	Habitat type * pH	2	0.002	4.01	0.02

Table S2. Results from two-way ANOVA showing the variation of the relative abundance of biofilm bacterial orders across different sites.

		df	Mean square	F value	P value
Sphingobacteriales	Habitat type	1	95.67	1.49	0.23
	pH	2	75.79	1.18	0.32
	Habitat type * pH	2	159.8	2.49	0.09
Flavobacteriales	Habitat type	1	11.9	0.31	0.57
	pH	2	229	6.07	0.006
	Habitat type * pH	2	634.8	16.8	<0.001
Oscillatoriales	Habitat type	1	191.7	9.89	0.003
	pH	2	169.3	8.74	0.001
	Habitat type * pH	2	127.9	6.60	0.004
Pleurocapsales	Habitat type	1	2.56	0.07	0.78
	pH	2	217.5	6.19	0.005
	Habitat type * pH	2	109.4	3.11	0.05
Vibrionales	Habitat type	1	1734.4	10.25	0.003
	pH	2	16.7	0.09	0.90
	Habitat type * pH	2	13.7	0.08	0.92
Cytophagales	Habitat type	1	56.83	14.03	<0.001
	pH	2	18.16	4.48	0.01
	Habitat type * pH	2	32.84	8.10	0.001
Rhodobacterales	Habitat type	1	2.10	0.61	0.43
	pH	2	1.11	0.32	0.72
	Habitat type * pH	2	19.01	5.52	0.009
Nostocales	Habitat type	1	228.1	15.25	<0.001
	pH	2	13.61	0.91	0.41
	Habitat type * pH	2	38.75	2.59	0.09
Alteromonadales	Habitat type	1	760.9	32.70	<0.001
	pH	2	106.3	4.56	0.01
	Habitat type * pH	2	107	4.59	0.01
Rhodospirillales	Habitat type	1	0.65	0.34	0.56
	pH	2	4.84	2.58	0.09
	Habitat type * pH	2	8.12	4.32	0.02
Rhodothermus_o	Habitat type	1	6.38	32.18	<0.001
	pH	2	0.59	2.98	0.06
	Habitat type * pH	2	0.44	2.22	0.12
Rhizobiales	Habitat type	1	0.25	0.96	0.33
	pH	2	1.64	6.17	0.005
	Habitat type * pH	2	4.12	15.54	<0.001

Planctomycetales	Habitat type	1	2.80	9.29	0.004
	pH	2	0.54	1.81	0.18
	Habitat type * pH	2	2.27	7.53	0.002
Verrucomicrobiales	Habitat type	1	1.45	1.51	0.22
	pH	2	2.67	2.79	0.077
	Habitat type * pH	2	8.31	4.34	0.022
Phycisphaerales	Habitat type	1	0.25	5.86	0.02
	pH	2	0.56	12.91	<0.001
	Habitat type * pH	2	0.16	3.72	0.03
Kordiimonadales	Habitat type	1	3.02	4.21	0.04
	pH	2	6.74	9.41	<0.001
	Habitat type * pH	2	2.31	3.22	0.05
Parvularculales	Habitat type	1	0.08	2.61	0.11
	pH	2	0.20	6.22	0.005
	Habitat type * pH	2	0.004	0.13	0.87
Balneola_o	Habitat type	1	1.64	3.78	0.06
	pH	2	1.59	3.66	0.03
	Habitat type * pH	2	1.63	3.75	0.03
Chromatiales	Habitat type	1	0.23	32	<0.001
	pH	2	0.05	6.96	0.003
	Habitat type * pH	2	0.10	13.68	<0.001
Myxococcales	Habitat type	1	0.002	0.52	0.47
	pH	2	0.03	7.74	0.001
	Habitat type * pH	2	0.01	2.71	0.08

Table S3. Results from two-way ANOVA showing the variation of the relative abundance of biofilm bacterial families across different sites.

		df	Mean square	F value	P value
Saprospiraceae	Habitat type	1	95.77	1.45	0.23
	pH	2	76.24	1.18	0.31
	Habitat type * pH	2	160	2.49	0.09
Flavobacteriaceae	Habitat type	1	13.8	0.37	0.54
	pH	2	220.3	5.94	0.006
	Habitat type * pH	2	600.6	16.22	<0.001
Pleurocapsa family	Habitat type	1	2.53	0.07	0.79
	pH	2	217.3	6.19	0.005
	Habitat type * pH	2	109.4	3.11	0.05
Vibrionaceae	Habitat type	1	1734.4	10.25	0.003
	pH	2	16.7	0.09	0.90
	Habitat type * pH	2	13.7	0.08	0.92
Rivulariaceae	Habitat type	1	225.5	15.24	<0.001
	pH	2	12.13	0.82	0.45
	Habitat type * pH	2	40.89	2.76	0.07
Pseudoalteromonadaceae	Habitat type	1	508.4	22.64	<0.001
	pH	2	99.8	4.44	0.02
	Habitat type * pH	2	99.7	4.44	0.02
Rhodobacteraceae	Habitat type	1	1.49	1.41	0.24
	pH	2	1.94	1.84	0.17
	Habitat type * pH	2	5.21	4.94	0.01
Porifericola family	Habitat type	1	10.50	11.31	0.002
	pH	2	2.01	2.17	0.13
	Habitat type * pH	2	4.26	4.59	0.01
Hyphomonadaceae	Habitat type	1	0.05	0.04	0.83
	pH	2	4.24	3.75	0.03
	Habitat type * pH	2	4.42	3.91	0.03
Planctomycetaceae	Habitat type	1	2.80	9.29	0.004
	pH	2	0.54	1.081	0.18
	Habitat type * pH	2	2.27	7.53	0.002
Rubricoccus family	Habitat type	1	5.11	44.70	<0.001
	pH	2	0.22	1.96	0.15
	Habitat type * pH	2	0.36	3.14	0.05
Erythrobacteraceae	Habitat type	1	4	16.64	<0.001
	pH	2	0.94	3.94	0.03
	Habitat type * pH	2	0.62	2.58	0.9

Sphingomonadaceae	Habitat type	1	0.28	1.41	0.24
	pH	2	0.73	3.67	0.03
	Habitat type * pH	2	2.23	11.12	<0.001
Planktothrix family	Habitat type	1	14.42	15.06	<0.001
	pH	2	14.04	14.66	<0.001
	Habitat type * pH	2	12.01	12.54	<0.001
Alteromonadaceae	Habitat type	1	9.72	16.23	<0.001
	pH	2	0.36	0.61	0.54
	Habitat type * pH	2	0.45	0.75	0.47
Phycisphaeraceae	Habitat type	1	0.12	4	0.05
	pH	2	0.20	6.72	0.003
	Habitat type * pH	2	0.03	1.30	0.28
Flammeovirgaceae	Habitat type	1	1.29	6.75	0.01
	pH	2	1.09	5.68	0.008
	Habitat type * pH	2	1.22	6.40	0.004
Alysiosphaera family	Habitat type	1	0.32	6.45	0.01
	pH	2	0.28	5.61	0.008
	Habitat type * pH	2	0.39	7.9	0.001
Cohaesibacteraceae	Habitat type	1	0.15	8.2	0.007
	pH	2	0.01	0.92	0.40
	Habitat type * pH	2	0.14	7.37	0.002

- 1 **Table S4.** Samples of “Boulder-Very low” and “Cliff-Ambient” sites formed the lowest nest while the
- 2 other samples are basically a subset of these.

Group	Rank order of nestedness
Boulder-Very low 1	16
Boulder-Very low 2	15
Boulder-Very low 3	3
Boulder-Very low 4	5
Boulder-Very low 5	23
Boulder-Very low 6	13
Cliff-Ambient 1	14
Cliff-Ambient 2	17
Cliff-Ambient 3	1
Cliff-Ambient 4	2
Cliff-Ambient 5	6
Cliff-Low 1	12
Cliff-Low 2	31
Cliff-Low 3	33
Cliff-Low 4	10
Cliff-Low 5	18
Cliff-Low 6	4
Cliff-Medium 1	25
Cliff-Medium 2	11
Cliff-Medium 3	7
Cliff-Medium 4	35
Cliff-Medium 5	32
Cliff-Medium 6	22
Boulder-Ambient 1	30
Boulder-Ambient 2	34
Boulder-Ambient 3	19
Boulder-Ambient 4	8

Boulder-Ambient 5	27
Boulder-Ambient 6	24
Boulder-Low 1	20
Boulder-Low 2	29
Boulder-Low 3	9
Boulder-Low 4	21
Boulder-Low 5	28
Boulder-Low 6	26

3

4